
Volume 61
Number 3
March 2010
ELSEVIER
MATERIALS
CHARACTERIZATION
An International Journal on Materials Structure and Behavior
EDITOR-IN-CHIEF
I. Baker
ASSOCIATE EDITORS
D.P. Field
D.W. Hetzner
I. Kaus
P.R. Munroe
J.D. Robson
1 μm
Published in Association with the International Metallographic Society
An Affiliate Society of ASM International®
www.elsevier.com/locate/matchar
ISSN 1044-5803

MATERIALS CHARACTERIZATION 61 (2010) 347–354

available at www.sciencedirect.com

ScienceDirect

www.elsevier.com/locate/matchar

Microstructural characterization of pipe bomb fragments

Otto Gregory[a,*], Jimmie Oxley[c], James Smith[c], Michael Platek[a], Hamouda Ghonem[b], Evan Bernier[c], Markus Downey[a], Christopher Cumminskey[a]
Sensors and Surface Technology Partnership Forensic Science Partnership

[a]Department of Chemical Engineering, University of Rhode Island, Kingston, RI, 02881, USA
[b]Department of Mechanical Engineering, University of Rhode Island, Kingston, RI, 02881, USA
[c]Department of Chemistry, University of Rhode Island, Kingston, RI, 02881, USA

ARTICLE DATA

Article history:
Received 22 May 2009
Received in revised form
17 December 2009
Accepted 22 December 2009

Keywords:
Pipe bomb
High strain rate loading
Steel microstructure

ABSTRACT

Recovered pipe bomb fragments, exploded under controlled conditions, have been characterized using scanning electron microscopy, optical microscopy and microhardness. Specifically, this paper examines the microstructural changes in plain carbon-steel fragments collected after the controlled explosion of galvanized, schedule 40, continuously welded, steel pipes filled with various smokeless powders. A number of microstructural changes were observed in the recovered pipe fragments: deformation of the soft alpha-ferrite grains, deformation of pearlite colonies, twin formation, bands of distorted pearlite colonies, slip bands, and cross-slip bands. These microstructural changes were correlated with the relative energy of the smokeless powder fillers. The energy of the smokeless powder was reflected in a reduction in thickness of the pipe fragments (due to plastic strain prior to fracture) and an increase in microhardness. Moreover, within fragments from a single pipe, there was a radial variation in microhardness, with the microhardness at the outer wall being greater than that at the inner wall. These findings were consistent with the premise that, with the high energy fillers, extensive plastic deformation and wall thinning occurred prior to pipe fracture. Ultimately, the information collected from this investigation will be used to develop a database, where the fragment microstructure and microhardness will be correlated with type of explosive filler and bomb design. Some analyses, specifically wall thinning and microhardness, may aid in field characterization of explosive devices.

1. Introduction

In the United States, pipe bombs are a common improvised explosive device. Construction is straightforward, and both metal and plastic pipes are readily available. Many of the pipe fillers are propellants which may include black powder, smokeless powder, photo and fireworks powder, and even match heads which can be purchased without special permit [1]. Over the years, law enforcement has developed robust protocols for processing bomb scenes and analytical procedures for identifying explosive residue, but chemical residue is not always recovered [2,3]. Generally, the recovered fragments are intermixed with a host of metal shards and debris characteristic of the chaotic scene of an explosion. A wealth of forensic information remains unexploited in terms of "metallurgical evidence" found in each pipe fragment. Such evidence is embodied in changes in the microstructure and microhardness of the pipe fragments. Metallurgical changes in armor steels have been extensively studied in order to estimate explosive loadings [4]. The degree of shock loading in plain carbon steel is reflected by pearlite and ferrite grain deformation, twinning, and slip band formation [5]. This study

* *Corresponding author*. Department of Chemical Engineering, 16 Greenhouse Rd, Kingston, RI, 02881, USA. Tel.: +1 401 874 2085.
E-mail address: gregory@egr.uri.edu (O. Gregory).

1044-5803/$ – see front matter
doi:10.1016/j.matchar.2009.12.017

attempts to correlate such microstructural features found in recovered steel pipe bomb fragments with the power and quantity of the propellant used, as well as other characteristics of the initial device [6]. The characterization included the application of quantitative stereology techniques to study the microstructural changes that occur in plain carbon-steel pipes due to high strain rate deformation and variations in microhardness obtained under different loading conditions. A correlation between pipe fragment microstructure, microhardness, and wall thinning with the pipes propellant filler may provide clues concerning the relative nature of the propellant in cases where chemical residue is not recovered.

2. Experimental

2.1. *Materials/Methods*

Commercially available, continuously welded, schedule 40 steel pipes [2 in. I.D. by 12 in. long (5 cm × 30.5 cm)] were used in this investigation. These galvanized AISI 1030 steel pipes nominally contain 0.3% carbon by weight and trace amounts of other impurities. Standard end caps were used at both ends of the threaded pipes and the pipes were usually initiated in a vertical orientation, with the detonator threaded through a hole drilled in the top end cap. To contain the fragments, pipes were initiated in 55-gallon (208.14 L) drums which were mostly filled with either sand or ground cornhusks. A cardboard sleeve was placed around the vertical pipe to ensure there was no direct contact between the pipe and the drum filler. Pipes were filled to volume (i.e. pour density) with black powder or one of the following smokeless powders: WC 870 (DB); IMR-PB (SB); Red Dot (DB); Winchester Action Pistol (DB); Bullseye (DB); where SB and DB indicate single (nitrocellulose) or double-base (nitrocellulose and nitroglycerin) powder, respectively. An improvised formulation made of sodium chlorate and aluminum chips as found in paint was also tested. Nitromethane, a high explosive, was used as a reference material. (Ref. [7] contains additional details related to the experimental procedure used here.)

Over 60 pipes were shot under the controlled conditions described above, and on average 87% of the pipe material was recovered. An effort was made to separate end cap pieces from those of the main body of the pipe, such that only those fragments from the main body of the pipe were selected for the microstructural analysis. Fragments from the end caps were not used in this study because they, and the threaded portion of the steel pipe, were already work hardened prior to use (Fig. 1).

2.2. *Pipe Thinning*

The extent of plastic deformation prior to fracture was determined by measuring the wall thickness of the fragments in the radial direction using Vernier calipers and comparing these measurements to those from the wall of an unexploded pipe. No special sample preparation was necessary to make these measurements; thus, it may be a field-adaptable technique. By comparing the ratio of the fragment wall thickness to that of the wall thickness of an unexploded pipe (Eq. (1)), the engineering radial strain, or plastic strain, prior to fracture was estimated [8]. A total of 10–40 fragments were analyzed, at least four wall thickness measurements per fragment, for each type of energetic filler. The seam region of the pipe was avoided because seam edges exhibited less ductility and the reduction in wall thickness was less pronounced than in other locations.

$$(a_0 - a_f) / a_0 = \varepsilon_p \tag{1}$$

where

a_0 initial wall thickness (unexploded) = 4.15 mm
a_f final wall thickness (exploded)
ε_p plastic strain.

2.3. *Microhardness*

A Wilson microhardness tester with a 200 g load was used for all microhardness measurements. The measurements were made across the through-thickness of the wall of as-received fragments. This provided considerable insight into the extent of work hardening in the individual fragments as a function of radial position. The procedure required that a series of indentations be made across the fragment through-thickness followed by a measurement of the length of each indentation (*L*). In this way, the Knoop hardness number (HK) was determined from the indenter load and the indentation length using the equation [9]:

$$HK = 14229^*(P / L^2) \tag{2}$$

where

P applied load (g)
L length of indentation in (μm).

2.4. *Microscopy*

Recovered pipe fragments were prepared for examination by scanning electron microscopy (SEM) and optical microscopy using standard metallographic preparation techniques [5]. A JEOL JSM5900LV SEM equipped with an energy dispersive X-ray analyzer (EDX) was used at magnifications between 200 and 5000× to determine the fine microstructural features and the size of the microhardness indentations. The fragments were sectioned using a water soluble oil-cooled diamond saw so that they would fit into a standard 1.25-inch (3.18 cm) diameter metallurgical mount. The fragments were cut in such a way that the cross section of the pipe wall could be viewed. The sectioned fragments were mounted in an Extec® two-part epoxy and polished using Extec® silicon carbide polishing discs. Successively finer grit papers were used, starting with 120 grit paper and progressing to 240, 400, 600 and 1200 grit paper. After lapping on the 1200 grit paper, the samples were polished with 3.0μm and 0.3μm Extec® alumina slurries. To reveal the final microstructure, the fragments were etched for 30–90s in nital (1 vol.% nitric acid (50–70%)/95 vol% absolute ethanol).

A reflection light microscope (Nikon Optifont 100) with bright-field illumination was used for all optical microscopies. Optical micrographs were captured using a Nikon Digital Sight DS-Fi1 high definition (5-megapixel CCD) color camera head with a DS-L2 controller operated by Nikon's NIS-Elements (version F2.20)

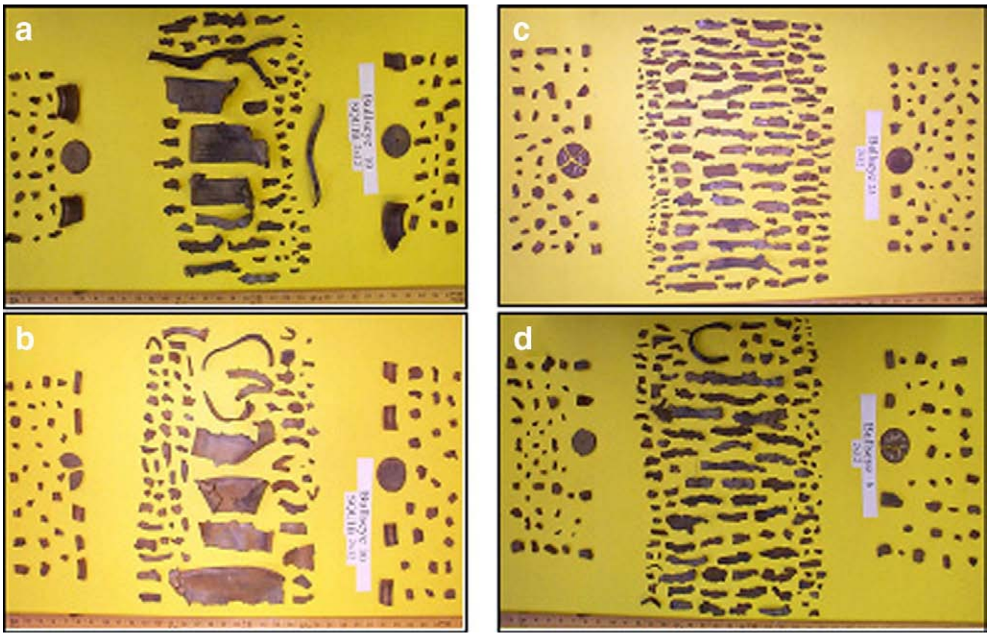

Fig. 1 – Photographs of pipe bomb fragments collected under controlled conditions: a.) Bullseye endcap detonation b.) Bullseye endcap detonation c.) Bullseye center detonation d.) Bullseye center detonation. On average 87% of the pipe material was collected.

software. Depending on the specific microstructural feature being analyzed, quantitative stereology was performed at magnifications of 20×, 50×, 100× or 200× [5]. A Sun Spark workstation running Princeton Gamma Tech (PGT) software was used to collect and analyze the images. The extent of plastic deformation in the α-ferrite grains and pearlite colonies, as measured by the aspect ratio in the digitally stored micrographs, was quantified utilizing the PGT metallography module. Deformation of the pearlite colonies was selected to follow the deformation trends instead of the α-ferrite grains because the dark pearlite colonies were more readily distinguished by the software than the light ferrite grains.

3. Results and Discussion

3.1. Thinning

Considerable thinning of the pipe wall was usually observed. Average fragment wall thickness is shown in Fig. 2, along with the associated plastic strain. Reduction in wall thickness was caused by plastic deformation that occurred prior to the rupture of the pipe material during explosion [10]. As the pressure wave propagated through the pipe, the material at the inner wall was placed in compression. This caused the material in the outer wall to expand (deform) biaxially and, as a result, the pipe became thinner and eventually ruptured. This plastic deformation prior to fracture increased as the power of each pipe bomb device increased. For example, black powder, the least powerful propellant in the study, caused the least plastic deformation prior to fracture. The fragments collected from explosions using black powder showed a 25% reduction in thickness, whereas pipes exploded with Bullseye smokeless powder, the most powerful propellant used, showed 61% reduction in wall thickness (Fig. 2).

3.2. Microscopy

Examination of pipe fragments using microscopy revealed specific detail on the extent of plastic deformation and the development of characteristic features in the steel microstructure. Fig. 3 shows the microstructure of an as-received (unexploded) steel pipe which was purposely over-etched (15 vol.% nital). Notice the visible boundaries of the α-ferrite grains (light phase) and the pearlite colonies (dark phase). It is evident from these micrographs that the individual grains are equiaxed, having approximately the same length and width. Scanning electron microscopy was used to observe the fine structure of the pearlite colonies. These colonies consist of alternating plates or lamellae of α-ferrite and cementite (Fe_3C)

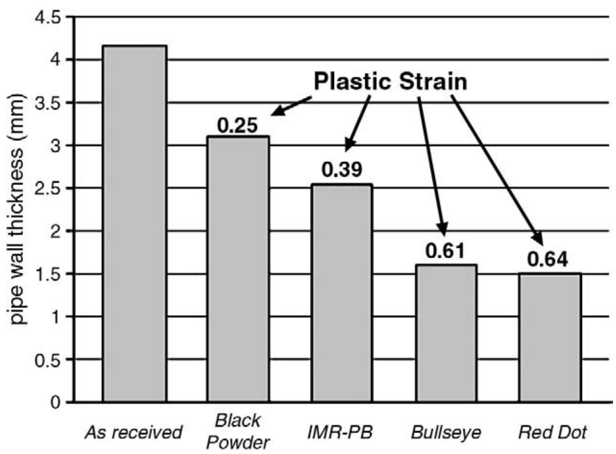

Fig. 2 – Changes in measured wall thickness of pipe bomb fragments as a function of filler (propellant) energy. Note corresponding plastic deformation prior to fracture.

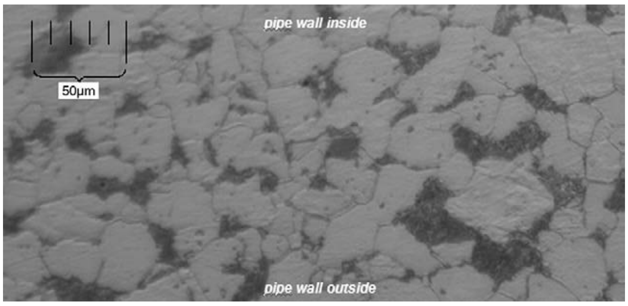

Fig. 3 – Optical micrograph of "as-received" plain carbon-steel pipe (transverse view — 500×). The dark phase is pearlite colonies and the light phase is α-ferrite grains. Grain boundaries are clearly visible due to over-etching of the sample (15% nital).

which are responsible for the scattering of visible light and resulting dark contrast of the colonies in the optical micrographs (Fig. 4).

Fig. 5 shows a micrograph of a fragment collected from a pipe filled with black powder. The pearlite colonies and α-ferrite grains are visibly deformed and elongated in the direction of the applied strain. As the power of the propellant filler increased, the deformation of the pearlite became more pronounced. This trend is shown in Fig. 6 for an improvised formulation of $NaClO_3$/Al. To quantify the extent of pearlite deformation, the average aspect ratio of the pearlite colonies from the various pipe bomb fragments was determined. An aspect ratio close to one represents features that are very symmetrical or equiaxed. The as-received pipe seen in Fig. 3 had average pearlite aspect ratios closer to 2 than 1. The aspect ratios of the pearlite colonies correlate well with the observed plastic deformation prior to pipe fracture. As expected, the more powerful fillers yielded larger pearlite aspect ratios (Fig. 7).

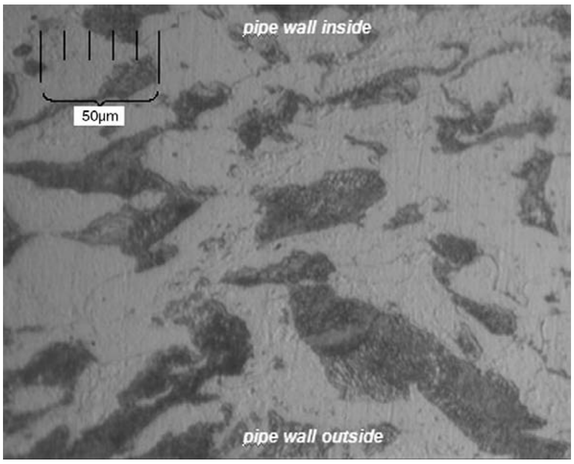

Fig. 5 – Optical micrograph of a recovered steel pipe bomb fragment with black powder used as the filler (transverse view — 200×). Note the deformation (elongation) of the pearlite (dark phase) and subsequent change in aspect ratio associated with the pearlite and α-ferrite relative to the as-received pipe (Fig. 4).

In the fragments collected from pipes using high-power fillers, twinning was observed along with elongation of both the α-ferrite grains and pearlite colonies. These characteristics were observed for Winchester Action Pistol 44, Red Dot, IMR-PB, Bullseye, and nitromethane as shown in Figs. 8, 9.A–9.C, 10.A–10.B, 11.A–11.C, and 12.A–12.B respectively. Normally, plastic deformation in body-centered cubic (BCC) metal occurs by slip, but deformation twins can occur in BCC metals and alloys at very low temperatures or at very high strain rates [10,11]. Therefore, the high-power propellants must have produced sufficiently high shock loading (pressure waves) within the walls of the pipe, prior to fracture, to

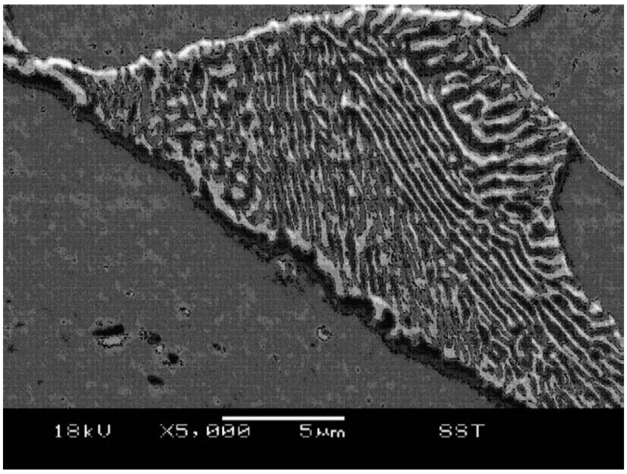

Fig. 4 – SEM micrograph of pearlite colony lamella in a steel pipe (5000×). The light phase is cementite (Fe_3C) and the dark phase is α-ferrite. [The lamella appears as a solid black phase in lower magnification micrographs as its structure encourages light scattering.]

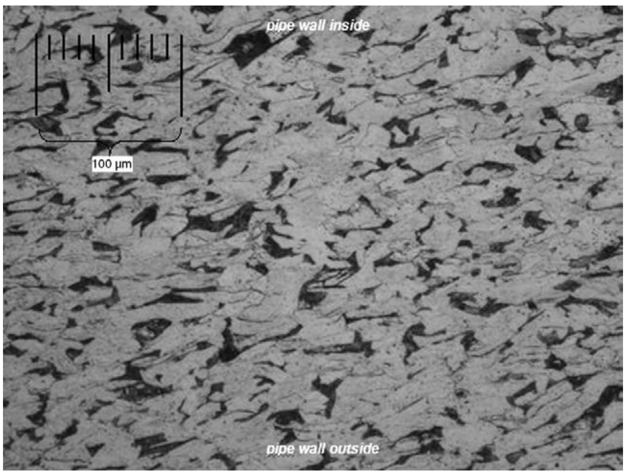

Fig. 6 – Optical micrograph of a recovered steel pipe bomb fragment with $NaClO_3$/Al used as the filler (200×). Note the deformation of the pearlite (dark phase).

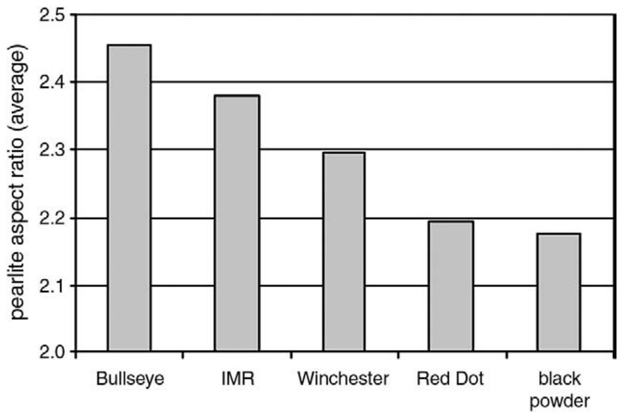

Fig. 7 – Relative plastic deformation of pearlite colonies in collected pipe bomb fragments prior to fracture, as evidenced by the changes in aspect ratio. Note the variation in aspect ratio as a function of filler (propellant) power.

induce twin plane formation in the steel pipe. The twin density was relatively low in most instances where twins were observed, due to random orientation of the pearlite colonies in the starting material. When high-power, high explosive fillers such as nitromethane were employed in this study, additional microstructural features were observed. The pearlite colonies were extremely distorted in continuous bands which extended well beyond a single grain or colony (Figs. 12.A–12.B). Fig. 12.A also reveals the presence of intersecting slip bands, or cross-slip bands, in the steel detonated with nitromethane.

A qualitative representation of the various threshold energy levels associated with the different propellants is shown in Fig. 13. Low-power propellant fillers, such as black powder, released enough energy to deform both the α-ferrite grains and pearlite colonies. Higher-power fillers, such as Winchester or

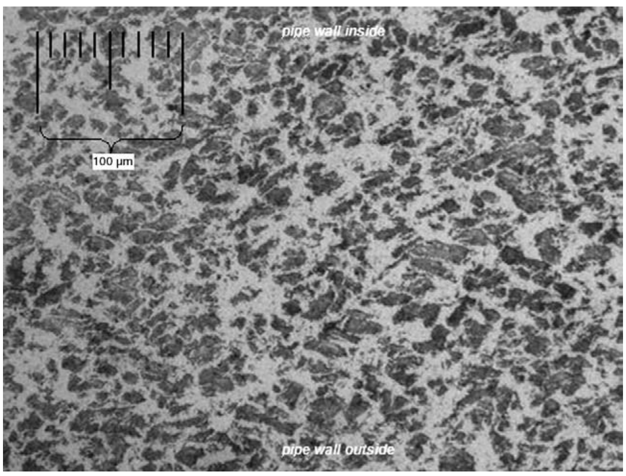

Fig. 8 – Optical micrograph of a recovered pipe bomb fragment with Winchester 44 used as the filler (transverse view — 200×). Note the deformation of the pearlite (dark phase) as well as the presence of twins in the microstructure.

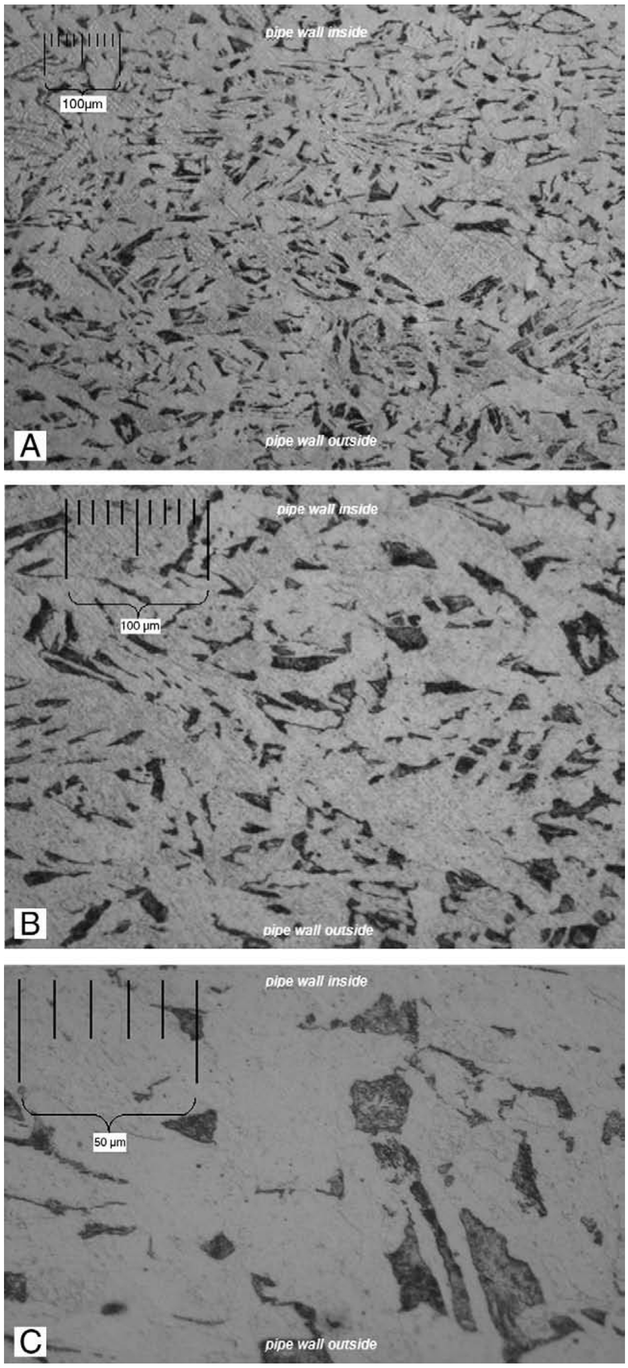

Fig. 9.A – Optical micrograph of a recovered steel pipe bomb fragment with Red Dot used as the filler (transverse view — 100×). Note the heavily deformed pearlite (dark phase). 9.B. Optical micrograph of a recovered steel pipe bomb fragment with Red Dot used as the filler (transverse view — 200×). Note the heavily deformed pearlite (dark phase) as well as the presence of twins in the microstructure. 9.C. Optical micrograph of a recovered steel pipe bomb fragment with Red Dot used as the filler (transverse view — 500×). Expanded view of twinning and deformed pearlite.

Red Dot, showed twin formation in addition to elongation of the pearlite colonies. In the most powerful devices, for example, employing IMR, Bullseye or nitromethane, the pearlite colonies

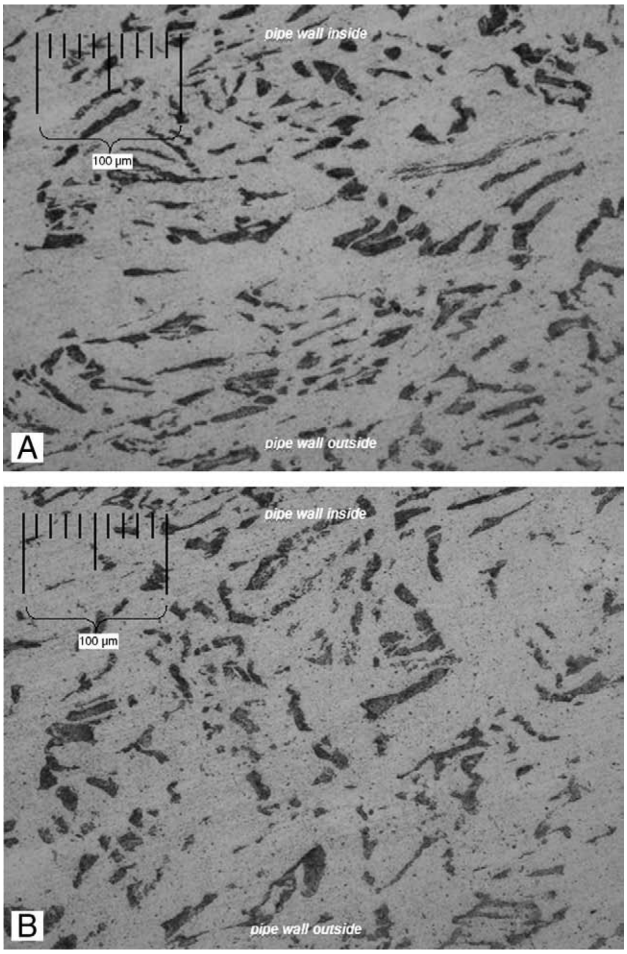

Fig. 10.A – Optical micrograph of a recovered steel pipe bomb fragment with IMR used as the filler (transverse view — 200×). Note the deformation of the pearlite (dark phase) and its overall distortion in continuous bands. 10.B. Optical micrograph of a recovered steel pipe bomb fragment with IMR used as the filler (transverse view — 200×). Note the deformation of the pearlite (dark phase) as well as the presence of twins in the microstructure.

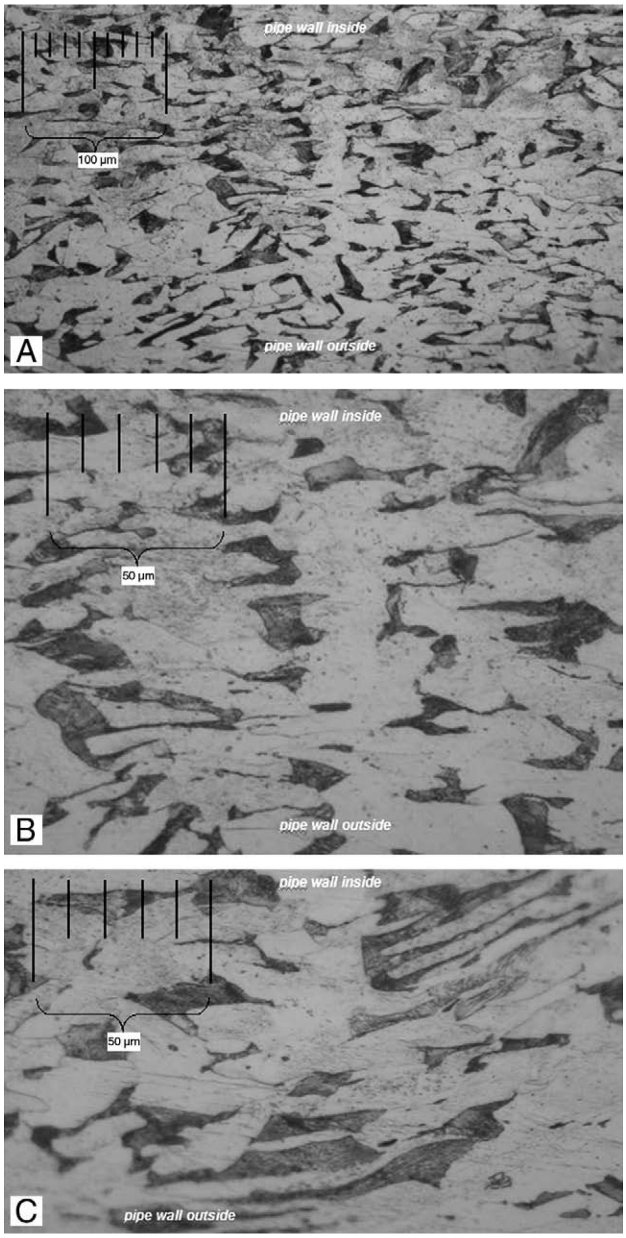

Fig. 11.A – Optical micrograph of a recovered steel pipe bomb fragment with Bullseye used as the filler (transverse view — 200×). Note the heavily deformed pearlite (dark phase) and its overall distortion in continuous bands, as well as the presence of twins in the microstructure. 11.B. Optical micrograph of a recovered steel pipe bomb fragment with Bullseye used as the filler (transverse view — 500×). Note the heavily deformed pearlite (dark phase) as well as the presence of twins in the microstructure. 11.C. Optical micrograph of a recovered steel pipe bomb fragment with Bullseye used as the filler (transverse view — 500×). Note the heavily deformed pearlite (dark phase) as well as the presence of twins in the microstructure.

were severely distorted and formed continuous bands extending beyond a single ferrite grain or pearlite colony. Fragment analysis from the pipe bomb detonated with the only high explosive, nitromethane, showed a significant number of slip bands.

3.3. *Microhardness*

The observed microstructural changes were accompanied by work hardening of the steel during the high strain rate conditions. The energy of the pressure wave created by the propellant was partially dissipated by the pipe material in the form of work hardening; i.e. the metal at the inner wall was compressed into the outer wall material. Microhardness test results were consistent with the degree of plastic deformation as determined from the physical thinning of the pipe fragment walls. Larger Knoop hardness values were associated with fragments produced from high-power propellants. Every filler used produced consistent Knoop hardness numbers with standard deviations less than 20 for the five points tested at the three locations tested; inside, middle and outside pipe wall. This result correlates well with the pearlite aspect ratios

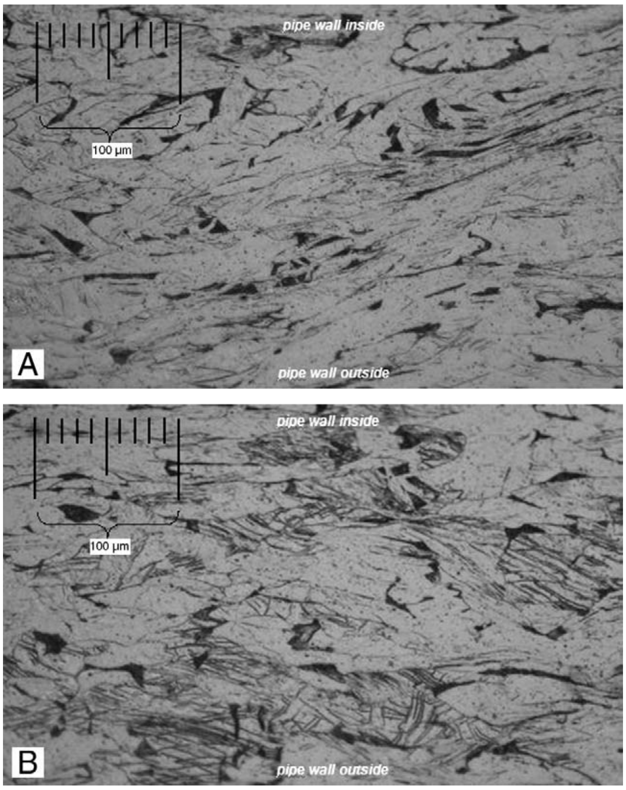

Fig. 12.A – Optical micrograph of a recovered steel pipe bomb fragment with nitromethane used as the propellant (transverse view — 200×). Note the heavily deformed pearlite (dark phase) as well as the presence of slip bands and twins in the microstructure. 12.B. Optical micrograph of a recovered steel pipe bomb fragment with nitromethane used as the propellant (transverse view — 200×). Note the heavily deformed pearlite (dark phase) as well as the presence of slip bands and twins in the microstructure.

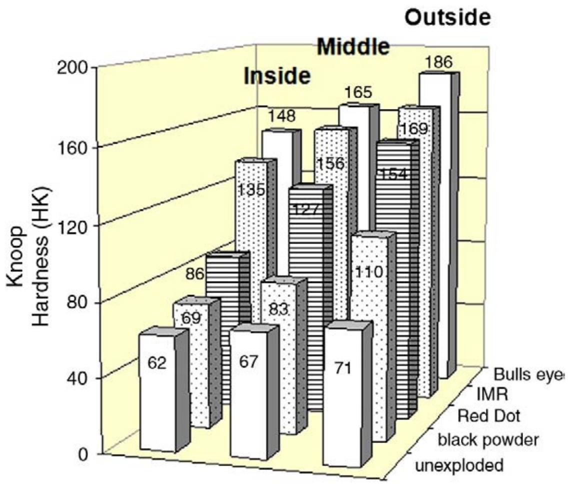

Fig. 14 – Microhardness variations of pipe bomb fragments as a function of radial position; i.e. microhardness variations within the wall of exploded pipes. Note the variation in microhardness with propellant energy.

determined from quantitative stereology, where more powerful explosive devices showed greater pearlite deformation (larger aspect ratios) and greater work hardening (microhardness numbers). A radial variation in microhardness was also observed i.e. microhardness numbers measured at the outer wall of the pipe fragments were typically larger than those measured at the inner wall. Fig. 14 illustrates the change in microhardness as a function of propellant energy and radial position. The work hardening was caused by the propagation of the pressure wave through the pipe wall and was enhanced by the compression of the material from the inner to the outer wall. Thus, the observed work hardening is greater at the outer wall than the inner wall of the pipe.

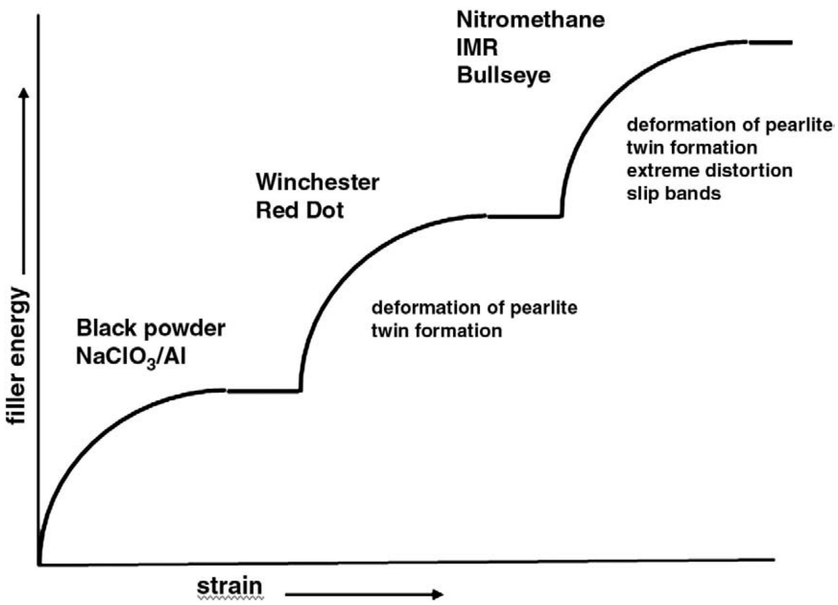

Fig. 13 – Microstructural changes observed in pipe bomb fragments collected after detonation.

4. Conclusions

More powerful, faster burning, propellants produced more plastic deformation in steel pipe bombs prior to fracture than lower power propellants. This can be shown by quantitative stereology and microhardness analysis of the pipe fragments recovered after the explosion. As the power of the propellant filler increased, the extent of work hardening in the pipe fragments also increased, as measured by microhardness. A radial variation in microhardness was observed, with larger Knoop Hardness values at the outer pipe wall than at the inner wall of the pipe fragments. Moreover, the recovered pipe fragments exhibited four distinct changes in microstructure, which also showed a strong correlation with the power of the propellant. The microstructural changes observed in the post-blast pipe fragments include (1) deformation of α-ferrite grains and pearlite colonies as evidenced by changes in aspect ratio, (2) twin formation, (3) distortion of pearlite colonies in continuous bands, and (4) formation of cross-slip bands. Quantitative stereology revealed that the average aspect ratio of the pearlite colonies in the recovered fragments increased with increasing filler energy. This trend was consistent with the work hardening effect determined from microhardness measurements of the fragments.

REFERENCES

[1] Arson and Explosives Incidents Report; Bureau of Alcohol, Tobacco, and Firearms: Dept. of Treasury: Washington D.C., 1997.

[2] A Guide for Explosion and Bombing Scene Investigation; J181869; U.S. Department of Justice: June, 2000.

[3] 25 Ways to Fight Terrorism. Prism — American Society of Engineering Education Journal Feb., 2002, p 27.

[4] Raftenberg MN, Krause CD. Metallographic observations of armor steel specimens from plates perforated by shaped charge jets. Int J Imp Eng 1999;23:757–70.

[5] Vander-Voort GF. Metallography, principles and practices. New York: McGraw Hill Book Co; 1984.

[6] Walsh GA, Inal OT, Romero VD. A potential metallographic technique for the investigation of pipe bombings. J Forens Sci 2003;48(5):945–60.

[7] Oxley JC, Smith JL, Resende E, Rogers E, Strobel RA, Bender EC. Improvised explosive devices: pipe bombs. J For Sci 2001;46(3):87–110.

[8] Mock W, Holt WH. Fragmentation behavior of Armco Iron and HF-1 steel explosive-filled cylinders. J Appl Phys 1983;54(5):2350.

[9] ASTM E384-00 Test Method for Microindentation Hardness of Materials, American Society for Testing and Materials International, Volume 03.01, W. Conshohocken, PA, 2003.

[10] Reed-Hill RE. Physical metallurgy principles. 3rd ed. Boston, MA: PWS Publishing Co; 1994.

[11] Callister WD. Materials science and engineering, an introduction. 6th ed. Hoboken, NJ: John Wiley and Sons; 1999.